EUROPEAN HEMATOLOGY ASSOCIATION
haematologica
Journal of the European Hematology Association

ALK-positive anaplastic large cell lymphoma with the variant RNF213-, ATIC- and TPM3-ALK fusions is characterized by copy number gain of the rearranged ALK gene

by Jo-Anne van de Krogt, Marlies Vanden Bempt, Julio Finalet Ferreiro, Nicole Mentens, Kris Jacobs, Ursula Pluys, Kathleen Doms, Ellen Geerdens, Anne Uyttebroeck, Pascal Pierre, Lucienne Michaux, Timothy Devos, Peter Vandenberghe, Thomas Tousseyn, Jan Cools, and Iwona Wlodarska

Haematologica 2017 [Epub ahead of print]

Citation: van de Krogt JA, Vanden Bempt M, Finalet Ferreiro J, Mentens N, Jacobs K, Pluys U, Doms K, Geerdens E, Uyttebroeck A, Pierre P, Michaux L, Devos T, Vandenberghe P, Tousseyn T, Cools J, and Wlodarska I. ALK-positive anaplastic large cell lymphoma with the variant RNF213-, ATIC- and TPM3-ALK fusions is characterized by copy number gain of the rearranged ALK gene. Haematologica. 2017; 102:xxx doi:10.3324/haematol.2016.146571

ALK-positive anaplastic large cell lymphoma with the variant *RNF213*-, *ATIC*- and *TPM3-ALK* fusions is characterized by copy number gain of the rearranged *ALK* gene

Jo-Anne van der Krogt,[1] Marlies Vanden Bempt,[1,2] Julio Finalet Ferreiro,[1] Nicole Mentens,[1,2] Kris Jacobs,[1,2] Ursula Pluys,[1] Kathleen Doms,[1] Ellen Geerdens,[1,2] Anne Uyttebroeck,[3] Pascal Pierre,[4] Lucienne Michaux,[1] Timothy Devos,[5] Peter Vandenberghe,[1,5] Thomas Tousseyn,[6] Jan Cools,[1,2] and Iwona Wlodarska[1]

[1]Center for Human Genetics, KU Leuven, Leuven, Belgium,

[2]Center for Cancer Biology, VIB, Leuven, Belgium,

[3]Department of Pediatrics, University Hospitals Leuven, Leuven, Belgium,

[4]Department of Hematology, Cliniques Sud Luxembourg, Arlon, Belgium,

[5]Department of Hematology, University Hospitals Leuven, Leuven, Belgium, and [6]Translational Cell and Tissue Research KU Leuven and Department of Pathology University Hospitals Leuven, Leuven, Belgium

JAvdK and MVB contributed equally to this work

Running head: Recurrent gain of *ALK* in ALK+ ALCL

Correspondence: Iwona Wlodarska; e-mail: iwona.wlodarska@uzleuven.be

Word count:

Abstract: 248

Text: 3851

Tables: 2

Figures: 4

Supplemental files : 1

Acknowledgements

The authors would like to thank Vanessa Vanspauwen and Emilie Bittoun for their excellent technical assistance, and Rita Logist for the editorial help. This study was supported by the concerted action grant from the K.U.Leuven no. 3M040406 (JAvdK, PV, TT, JC and IW) (http://www.kuleuven.be/), research grants from the FWO Vlaanderen (G081411N to TT) and “Stichting tegen Kanker” (PV) (http://www.kanker.be/). MVDB holds a SB Fellowship of the Research Foundation-Flanders. PV is a senior clinical investigator of the FWO-Vlaanderen. TT holds a Mandate for Fundamental and Translational Research from the “Stichting tegen Kanker” (2014-083).

ABSTRACT

ALK positive anaplastic large cell lymphoma is characterized by 2p23/*ALK* aberrations, including the classic t(2;5)(p23;q35)/*NPM1-ALK* rearrangement present in ~80% of cases and several variant t(2p23/*ALK*) occurring in the remaining cases. The *ALK* fusion partners play a key role in the constitutive activation of the chimeric protein and its subcellular localization. Using various molecular technologies, we have characterized ALK fusions in eight recently diagnosed anaplastic large cell lymphoma cases with cytoplasmic-only ALK expression. The identified partner genes included *EEF1G* (one case), *RNF213/ALO17* (one case), *ATIC* (four cases) and *TPM3* (two cases). Notably, all cases showed copy number gain of the rearranged *ALK* gene, which is never observed in *NPM1-ALK*-positive lymphomas. We hypothesized that this could be due to lower expression levels and/or lower oncogenic potential of the variant ALK fusions. Indeed, all partner genes, except *EEF1G,* showed lower expression in normal and malignant T cells, in comparison with *NPM1.* In addition, we investigated the transformation potential of endogenous Npm1-Alk and Atic-Alk fusions generated by CRISPR/Cas9 genome editing in Ba/F3 cells. We found that Npm1-Alk has a stronger transformation potential than Atic-Alk, and we observed a subclonal gain of *Atic-Alk* after a longer culture period, which was not observed for *Npm1-Alk*. Taken together, our data illustrate that lymphomas driven by the variant ATIC-ALK fusion (and likely by RNF213-ALK, and TPM3-ALK), but not the classic NPM1-ALK, require an increased dosage of the *ALK* hybrid gene to compensate for the relatively low and insufficient expression and signaling properties of the chimeric gene.

Introduction

Anaplastic large cell lymphoma (ALCL) expressing the anaplastic lymphoma kinase (ALK) (ALK+ ALCL) is a rare but well-defined subtype of peripheral T-cell lymphoma (PTCL).[1] It accounts for approximately 3% of all non-Hodgkin lymphomas (NHL) in adults, for 10-15% of pediatric lymphomas and 60-80% of all ALCLs. ALK+ ALCL is hallmarked by various 2p23/*ALK* chromosomal rearrangements leading to an aberrant expression and constitutive activation of the ALK tyrosine kinase. The most prevalent lesion occurring in more than 80% of ALK+ ALCL is t(2;5)(p23;q35) involving *ALK* and *NPM1* (nucleophosmin) genes, respectively.[2] The translocation generates a chimeric protein comprising the N-terminus oligomerization domain of NPM1 and the C-terminus of ALK, including its intracellular tyrosine kinase domain.[2] The fusion acts as an oncogene and its transforming potential was proven in a number of *in vitro* and *in vivo* studies.[3-5] The remaining ALK+ ALCL cases harbor variant 2p23/*ALK* rearrangements affecting at least nine partners genes: *TPM3* (1q21.3; previously assigned to 1q25[6]), *ATIC* (2q35), *TFG* (3q12.2), *TRAF1* (9q33.2), *CLTC* (17q23.1), *ALO17/RNF213* (17q25.3), *TPM4* (19p13.12), *MYH9* (22q12.3) and *MSN* (Xq12).[7] The partners play a key role in the constitutive activation of the chimeric protein by mediating its oligomerization and determine subcellular localization of ALK fusion (cytoplasmic and nuclear, in NPM1-ALK positive cases, and cytoplasmic-only or membranous, in variant fusions)[8,9]. In addition, they impact a range of biological activities of ALK chimeras, including proliferation, transformation and metastatic capacities.[10,11] Comparative analysis of biological properties of ALK oncoproteins, however, is hampered by the relative low frequency of particular variant ALK fusions.

Interestingly, *ALK* rearrangements have been also detected in large B-cell lymphoma and various tumors of mesenchymal and epithelial origin, including inflammatory myofibroblastic tumors, lung cancer, esophageal squamous cell carcinoma and others.[7] Notably, the same ALK fusions, such as TPM3-ALK, TPM4-ALK, TFG-ALK, SEC31A-ALK, ATIC-ALK, CLTC-ALK and EML4-ALK occur in ALK+ malignancies of different cell of origin highlighting the crucial role of ALK in tumorigenesis.[7,12] These findings prompted development of new therapeutic strategies in ALK+ tumors. Particularly important is the recent discovery of specific ALK tyrosine inhibitors.[13,14] One of them, crizotinib, has proven to have clinical efficacy in treatment of ALK+ non-small cell lung cancer and ALCL.[15,16]

Here, we report molecular characterization of ALK fusions in eight ALK+ ALCL cases exhibiting a cytoplasmic-only ALK staining pattern recently diagnosed in our institution. Intriguingly, all cases

analyzed by fluorescence *in situ* hybridization (FISH) at time of diagnosis revealed copy number gain of the rearranged *ALK* gene.

Methods

Case selection

Eight cases of ALK+ ALCL with a cytoplasmic-only expression of ALK and available bioarchived material were selected from the database of the Center for Human Genetics and Department of Pathology, Universisty Hospital of the KU Leuven, Belgium. Morphology, immunophenotype and clinical records of the reported cases were reviewed. The institutional review board "Commissie Medische Ethiek" of the University Hospital approved this retrospective study and they renounced the need for written informed consent from the participants (S56799, ML10896: 12/08/2014).

Cytogenetics and FISH

Conventional G-banding chromosomal analysis and FISH analysis followed routine protocols. The probes applied on patient material and Ba/F3 cell lines are listed Supplemental Table 1. Non-commercial probes were directly labeled with SpectrumOrange- and SpectrumGreen-d-UTP (Abbot Molecular, Ottignies, Belgium) by random prime labeling. FISH images were acquired with a fluorescence microscope equipped with an Axiophot 2 camera (Carl Zeiss Microscopy, Jena, Germany) and a MetaSystems Isis imaging system (MetaSystems, Altussheim, Germany).

Array-based genomic hybridization (aCGH)

Total genomic DNA was isolated from frozen lymphoma samples using standard procedures. High-resolution aCGH was performed using the Affymetrix Cytoscan HD arrays (www.affymetrix.com) and followed the manufacturer protocols. Downstream data analysis of copy number alterations was conducted using the software ArrayStudio, version 6.2 (www.omicsoft.com).

Cell culture and growth curves

Ba/F3 cells constitutively expressing Cas9 (Ba/F3 Cas9) were generated using a retroviral expression vector containing a Cas9 expression cassette (Supplemental Figure 1). Ba/F3 Cas9 cells

were cultured with IL3 in RPMI medium + 10% FBS before and after electroporation. For growth curves, viability and proliferation were measured on a Guava flow cytometer (Merck Millipore, Darmstadt, Germany) for several consecutive days.

Quantitative RT-PCR (QRT-PCR)

QRT-PCR with the GoTaq qPCR Master Mix (Promega, Madison, Wisconsin) was used to analyze relative mRNA expression of two *Alk* partner genes (*Npm1* and *Atic*) in Ba/F3 Cas9 cells. Mouse Hprt1 and Rpl4 were used as an internal control. Primers are listed in Supplemental Table 2. All samples were run in triplicate and data were analyzed with the comparative Ct (ΔΔCt) method.

CRISPR/Cas genome editing

gRNAs were designed using the CRISPR design tool of the Zhang lab (crispr/mit.edu) (Supplementary Table 3). gRNAs were cloned into an expression plasmid (pX321, derived from pX330, Zhang lab; Supplemental Figure 2). Electroporations of Ba/F3 Cas9 cells were carried out using a Gene Pulser Xcell electroporation system (Biorad, Hercules, California). After electroporation, cells were kept in RPMI medium + 10% FBS + IL3 for 3 days before IL3 depletion was carried out.

Other applied techniques, including the 5' Rapid Amplification of cDNA Ends Polymerase-Chain-Reaction (RACE-PCR), Low Coverage Full Genome Sequencing (LCFGS), Targeted Locus Amplification (TLA) and Nested Reverse-Transcription Polymerase-Chain-Reaction (RT-PCR) are briefly described in Supplemental Methods.

Results

Clinical and pathological features

Relevant clinical and pathological features of the reported cases of ALK+ ALCL are shown in Table 1. There were two children (a 5 year-old boy and a 13 year-old girl) and six adults (two female and four males) in age ranging from 49 to 78 years (mean 64.8 year). All patients presented with lymph node involvement and one displayed additional skin lesions [stages I (cases 3 and 4), II (cases 5 and 8), III (cases 2 and 7) and IV (cases 1 and 6)]. Five adult patients (cases 2-6) were treated with

chemotherapy (CHOP), reached complete remission (CR) and are alive. The sixth adult patient (case 7) initially diagnosed as classical Hodgkin lymphoma, was treated with ABVD and radiotherapy, and also reached CR. He relapsed very recently (after 165 months) and died due to disease-related complications after the 3rd course of CHOP. Two other patients also experienced more aggressive course: one (case 2) achieved a second CR after DHAP and the first pediatric patient (case 1) initially treated according to the ALCL99 protocol, experienced three relapses. He achieved CR after treatment with crizotinib and allogenic stem cell transplantation but died 72 months after diagnosis due to severe GVHD and respiratory failure. The second pediatric patient (case 8) got 6 cycles of polychemotherapy (ALCL99) and remains in CR.

Histopathology showed an anaplastic lymphoid cell proliferation with characteristic hallmark and doughnut cells in all cases. The immunophenotype of the individual tumors is shown in Table 1 and illustrated in Supplemental Figure 3. All cases were CD30 positive, expressed a CD4+ or null cell phenotype in conjunction with variable cytotoxic markers, and overexpressed ALK1 in a strictly cytoplasmic pattern. The stromal infiltrate was prominent in all cases with a variable amount of histiocytes and/or neutrophils.

Cytogenetic and molecular studies

Case 1. Cytogenetic analysis showed a complex karyotype with del(2)(p23) (Table 2). FISH with LSI ALK demonstrated a break apart pattern with the green (5'*ALK*) signal on del(2)(p23) and two red (3'*ALK*) signals on a marker chromosome of postulated chromosome 11 origin (Figure 1A). Whole chromosome painting proved that der(11) indeed harbors the duplicated fragment of chromosome 2 inserted at 11q. The t(2p23/*ALK*) rearrangement was further investigated using the 5' RACE PCR approach. The analysis identified an in-frame fusion transcript in which exon 8 of *EEF1G,* the gene located at 11q12.3, was fused to exon 20 of *ALK* (Figure 1B). More precisely, the fusion joined nucleotide 1161 of *EEF1G* (NCBI ref NM-001404), corresponding to an intronic region between exons 8 and 9, with nucleotide 4226 of *ALK* (NM-004304) situated in exon 20. The *EEF1G-ALK* fusion was subsequently confirmed by Sanger sequencing of the fragment obtained by nested RT-PCR (Figure 1B) and by FISH using probes for 5'*EEF1G* and 3'*ALK* (not shown). Array CGH analysis demonstrated the 3'*ALK*-involving gain of 2p23.2p25.3 and the *EEF1G*-affecting gain of 11q11q13.4 (Figure 1C-D). In addition, gain of five other regions, loss of three large regions, including 9p21.3p24.3/*CDKN2A/B,*

and three microdeletions were detected (Figure 1C; Table 1). Interestingly, the focal deletion at 8q24.21 covered of ~280 kbp sequences flanking the centromeric border of *MYC*. The loss was confirmed by FISH with LSI MYC: one of two apparently normal looking chromosomes 8 [der(8)] revealed a significantly diminished red signal (Figure 1A).

Case 2. Cytogenetic analysis was unsuccessful. Interphase FISH with LSI ALK showed a break apart pattern associated with gain of up to seven red (3'*ALK*) signals (Figure 2A). The FISH pattern suggested a diploid and tetraploid status of abnormal cells. The *ALK* rearrangement was further investigated using LCFGS. The analysis identified the *RNF213-ALK* fusion (supported by at least 8 read pairs) where the exon 8 of *RNF213* is fused to exon 20 of ALK, resulting in an in-frame fusion transcript equal to the previously described cases (Figure 2B).[6,17,18] The fusion and its gain were confirmed by FISH (Figure 2A). The performed aCGH analysis demonstrated the *ALK*- and *RNF213*-associated gain of 2p23.2p25.3 and 17q23.3q25.3, respectively (Figure 2C-D). In addition, aCGH detected gain of six other regions and loss of three regions, all listed in Table 2. Notably, breakpoints of the amplified 4p12p16 and 5q33.3q35.3 regions affected the *RNF212*/4p16 and *ITK*/5q33.3 genes, respectively. FISH with the respective break apart (BA) probes (Supplemental Table 1) confirmed the unbalanced rearrangement and partial gain of both genes. Further FISH with the probes for 5'*RNF212* and 3'*ITK* showed multiple, but not colocalized signals, precluding the *RNF212-ITK* hybrid gene (data not shown). Unfortunately, LCFGS has not identified any fusion of *RNF212* and *ITK.*

Cases 3-6. The cases were not subjected to cytogenetic analysis. FISH with LSI ALK applied on formalin fixed paraffine embeded (FFPE) material confirmed *ALK* rearrangement and displayed presence of 3-7 red (3'*ALK*) signals in all cases (Table 2, Figure 3A). Although a number of fused (F), red (R) and green (G) signals in analyzed cells varied, all cases showed a clear predominance of the red signals and variations of the 1F1G3R pattern. As a similar pattern was observed in *ATIC-ALK*-positive lymphoma[19], we examined at first the status of this gene. FISH with the ATIC BA assay revealed a break apart pattern and presence of extra 5'*ATIC* signals in all four cases (Figure 3B). Subsequent FISH with the 5'*ATIC* and 3'*ALK* probes demonstrated 3-5 fused signals per cell confirming the *ATIC-ALK* rearrangement and gain of the chimeric gene in all four cases (Figure 3C).

Case 7. The biopsy taken at time of relapse (2016) showed a complex diploid karyotype with a presumed ins(1;?)(q21;?) and ider(1)(q10) containing a duplicated 1q arm of ins(1;?)(q21;?) and del(2)(p23) (Table 2, Figure 3D). Interphase FISH with LSI ALK revealed the 1F1G3R pattern (Figure 3E), like in *ATIC-ALK* positive cases. Considering that the 1q21 breakpoint merges with localization of *TPM3*, the known *ALK* partner,[6] a possible involvement of this gene was investigated by FISH with the designed TPM3 BA assay (Supplemental Table 1). Neoplastic cells revealed the 1F3(RsepG) pattern postulating rearrangement of *TPM3* due to ins(1;2)(q21.3;p23p25) (Figure 3F). The *TPM3-ALK* fusion was subsequently confirmed by FISH using the 5'*TPM3*/3'*ALK* probes. In the next step, we revised the diagnostic sample (the case was initially misdiagnosed as classical Hodgkin lymphoma), in which cytogenetic analysis identified rare hypertetraploid cells with i(1)(q10) and del(2)(p23) (Table 2). FISH with LSI ALK (Figure 3G), TPM3 BA (Figure 3H) and the 5'*TPM3*/3'*ALK* probes (Figure 3I) demonstrated presence of the *TPM3-ALK* rearrangement and copy number gain of the ALK fusion already at time of diagnosis (2002).

Case 8. Cytogenetic analysis identified only one abnormal (near tetraploid) metaphase cell harboring five copies of chromosome 2 (Table 2). LSI ALK applied on this chromosome spread hybridized with all chromosomes 2: one showed a fused signal and other four were marked by red signals (Fig 3J). The abnormal FISH pattern (1-2F4R) was detected in 11% of interphase cells. Loss of the 5'*ALK* sequences suggested a focal interstitial del(2)(p23p23) leading to a novel fusion of *ALK* with a gene located at the centromeric breakpoint of the deletion. To identify a potential partner gene, we used TLA approach. Unexpectedly, the analysis identified the *TPM3-ALK* fusion with the breakpoints at the intron 7 of *TPM3* and the intron 19 of *ALK* (Supplemental Figure 4). FISH confirmed the *TPM3* rearrangement, which was associated with loss of the 3'*TPM3* sequences, and showed that four out of five chromosomes 2 harbor one copy of *TPM3-ALK* (Figure 3K-L). Altogether, we identified a cryptic insertion of the 5'*TPM3* into the rearranged *ALK* locus, loss of the 5'*ALK* and 3'*TPM3* sequences, and gain of two copies of *TPM3-ALK* in tetraploid neoplastic cells.

Functional studies

Gain of the *EEF1G-, RFN213-, ATIC-* and *TPM3-ALK* hybrid genes found in the present cases contrasts with a constant occurrence of a single copy of *NPM1-ALK* in t(2;5)-positive ALCL.[20-22] We

hypothesized that ALCLs harboring the variant rearrangements compensate an insufficient expression of the ALK fusions (driven by relatively weak promoters of the partner genes) by an increased dosage of the chimeric gene. To validate this concept, we analyzed expression levels of *NPM1, EEF1G, RNF213, ATIC and TPM3* in various normal lymphoid cells and T-cell malignancies using previously generated RNAseq data.[23,24] The analysis revealed a significantly lower (p-value <0.001) expression of *RNF213, ATIC* and *TPM3* in all samples when compared to *NPM1* (Figure 4A). In contrast, expression of *EEF1G* was similar to that of *NPM1*. Based on these findings, we hypothesized that oncogenic transforming properties of the three variant ALK fusions, RFN213-ALK, ATIC-ALK and TPM3-ALK, could be lower than the strong NPM1-ALK kinase. To validate our hypothesis, we attempted to generate the Npm-Alk and Atic-Alk fusions in the genome of Ba/F3 cells using CRISPR/Cas9 genome editing. The expression level of Npm1 is around 50-fold higher than the expression level of Atic in this cell line, making it a suitable model to test our hypothesis (Figure 4B). We designed a gRNA targeting exon 20 of *Alk* and gRNAs targeting *Npm1* and *Atic* in regions corresponding to the breakpoints observed in our patient samples (Figure 4C). gRNAs targeting *Alk* and a fusion partner were simultaneously introduced in Ba/F3 Cas9 cells by electroporation. Upon IL3 depletion, both endogenous Alk fusions were able to transform the Ba/F3 Cas9 cells, although cells harboring an endogenous Atic-Alk fusion needed more time to recover from the IL3 depletion (Figure 4D). In addition to the slower transformation rate, cells harboring an endogenous Atic-Alk fusion presented with a lower growth rate after transformation than cells with an endogenous Npm1-Alk fusion (Figure 4E). FISH demonstrated the presence of one copy of the *Npm1-Alk* and *Atic-Alk* chimeric genes per cell in the respective cell lines (Figure 4F-G). After keeping the cells in culture for three months, we observed gain of 1-3 copies of the *Atic-Alk* fusion gene in approximately 20% of the cells. In contrast, the *Npm1-Alk* cell line kept a single copy of the chimeric gene in all cells (Figure 4H). Altogether, these data demonstrate that the Npm1-Alk fusion is a more potent driver of proliferation than Atic-Alk in Ba/F3 cells, and that the expression level of the fusion partner is a key factor in the transformation potential of the oncogenic fusions.

Discussion

Our study provided evidence that ALCL driven by at least three variant *ALK* fusions, *RNF213-ALK, ATIC-ALK* and *TPM3-ALK*, is characterized by a copy number gain of the *ALK* hybrid gene. Gain of

RNF213-ALK was already observed by us in the previously reported case of ALK+ ALCL, harboring two copies of der(17)t(2;17)(p23.2;q25.3)/*RNF213(ALO17)-ALK*.[17] Genetic mechanisms underlying amplification of *RNF213-ALK* in case 2, however, remain unknown. Notably, the four *ATIC-ALK*-positive cases presented here, as well as all reported *ATIC-ALK* cases documented by FISH,[19,25-27] showed extra copies of the chimeric gene. We previously documented that the *ATIC-ALK* fusion is generated by a pericentric inv(2)(p23q35) and is constantly accompanied by isochromosome 2q (derivative of inv(2)) comprising two extra copies of *ATIC-ALK*.[19,25] Based on these data, we presume that the reported cases here also carry inv(2)(p23q35) and 1-3 copies of ider(2q). Intriguingly, a similar mechanism of gain of ALK hybrid emerged to underpin the *TPM3-ALK* rearrangement detected in case 7. The fusion was likely created by insertion of 3'*ALK*/2p23p25 at 1q21.3/*TPM3* and gained by a subsequent formation of ider(1)(q10). In the second *TPM3-ALK*-positive case, however, the chimeric gene was produced by a cryptic insertion of the 5'*TPM3* into the rearranged *ALK* locus and gained by a duplication of the der(2), like in the case reported by Siebert et al.[28] Notably, one more informative case with *TPM3-ALK* also presented with 2-3 copies of the 3'*ALK*.[29] Lamant et al.[6], who originally described the TPM3-ALK fusion in ALK+ ALCL, linked it to t(1;2)(q25;p23). Considering, however, an opposite transcriptional orientation of both genes, generation of the in-frame *TPM3-ALK* fusion requires more complicated events, as illustrated in the present and previously reported cases.[28]

Altogether, our genetic findings supported by the published data,[17,19,26-29] highlight a strong association of *RNF213-ALK, ATIC-ALK* and *TPM3-ALK* with a copy number gain of the chimeric gene. A spectrum of such *ALK* fusions is probably broader, but a frequent lack of cytogenetic and/or FISH data hampers their identification. These observations contrast with ALCL driven by *NPM1-ALK*[20-22] and at least three variant fusions, *CLTC-ALK*[17], *TPM4-ALK*[30,31] and *TRAF1-ALK*[27,32], shown to carry a single copy of the ALK hybrid gene. We initially included to the former category also the novel *EEF1G-ALK* variant found to be duplicated on der(11). Given, however, that two recently published ALCL cases with *EEF1G-ALK* did not show copy number gain of the ALK fusion gene,[33] duplication of *EEF1G-ALK* in our case was likely associated with progression of the disease, similar to a case of leukemic ALK+ ALCL with extra copy of *NPM1-ALK.*[34] This conclusion is additionally supported by our other data illustrating a strong expression of *EEF1G* in normal and malignant T cells, similar to that of *NPM1*. Thus, there is no reason why the EEF1G-ALK fusion gene would require an increased copy number.

In contrast, expression of *RNF213, ATIC* and *TPM3* in lymphoid cells was significantly lower than *NPM1* and *EEF1G.* These findings support the concept that ALCL driven by the *RNF213-ALK, ATIC-ALK* and *TPM3-ALK* fusions might require an increased dosage of *ALK* chimeric gene to compensate an insufficient expression of *ALK* in neoplastic cells. To test if the best documented Atic-Alk fusion is indeed less transforming than the Npm1-Alk fusion, we generated the *Npm1-Alk* and *Atic-Alk* fusion genes by inducing Cas9 mediated chromosomal rearrangements in Ba/F3 cells. Growth properties of these engineered cells showed that the transformation potential of *Atic-Alk* is significantly lower when compared to *Npm1-Alk*, likely due to a lower expression level of *Atic*. Interestingly, the tendency of the *Atic-Alk*-positive Ba/F3 cells to gain extra copies of the *Atic-Alk* chimeric gene recapitulates the events observed in the original tumors and confirms the selective pressure of the cells to acquire additional copies of the *Atic-Alk* fusion. We also attempted to generate an endogenous *Rnf213-Alk* fusion, but since *Rnf213* is very lowly expressed in Ba/F3 cells, this fusion could not transform the cells. *Tpm3* was not included in the functional studies, since it was only recently added to the study. Of note, Giuriato et al.[35] previously showed that in conditional knock-in mice both TPM3-ALK and NPM1-ALK could induce B-cell lymphoma/leukemia with a similar disease latency. In these transgenic mice, however, the expression levels of both ALK fusions were similar, since their expression was driven by an external promoter. This could explain the observed equal tumorigenic potential of both ALK fusions.

The novel *EEF1G-ALK* fusion identified by us in a child with ALK+ ALCL extends the already long list of *ALK* fusion partners comprising approximately 20 genes.[7] The very recent report of two pediatric patients with *EEF1G-ALK*[33] indicates that the fusion is recurrent and strongly associated with pediatric ALK+ ALCL. *EEF1G,* located at 11q12.3, has 10 exons encoding for an eukaryotic translation elongation factor 1 gamma. Together with α, β and δ subunits, it forms the eukaryotic elongation factor complex, which is predominantly involved in protein biosynthesis with an elongation of the polypeptide chains.[36,37] EEF1G comprises a glutathione transferase (GST)-like N-terminus domain and a C-terminus (CT) domain.[37] Although all four subunits of the elongation factor complex are highly expressed in most eukaryotic cells, the role of human EEF1G is poorly understood. Notably, an increased expression of *EEF1G* has been detected in various human carcinomas.[37-40] It has been suggested that overexpression of EEF1G stimulates the overgrowth of neoplastic cells.[41] In the present case of ALK+ ALCL, exons 1 to 8 of *EEF1G* are fused to exon 20-29 of *ALK,* resulting in a

chimeric protein with the complete GST-like-N-terminal domain and part of the CT domain of EEF1G, fused to the complete intracellular protein tyrosine kinase (PTK) domain of ALK (Figure 2B). Even though the complete PTK domain is involved, the ALK fragment contains the final 513 amino acids, which is shorter in comparison to the fragment involved in most other ALK-fusions, containing the final 563 amino acids.[42] Of note, both cases reported by Palacios et al.[33], revealed breakpoints within intron 7 of *EEF1G* and intron 20 of *ALK*. As the fusions were identified by RNAseq, genetic mechanisms underlying these rearrangements are unknown. The postulated t(2;11)(p23;q12.3), however, is unlikely, because of an opposite transcriptional orientation of both genes, similar to *TPM3* and *ALK* (www.ensembl.org). Functional studies performed by the authors provided evidence of the dimerization properties of the EEF1G-ALK fusion, constitutive activation of ALK kinase and its strong oncogenic potential similar to that of NMP1-ALK.

Our patient with *EEF1G-ALK* experienced an unfavorable and fatal clinical course. Although ALK+ ALCL has a relatively good prognosis, chemoresistant and aggressive forms of this lymphoma, recurrently featured by *MYC* aberrations, have been recurrently reported.[32,43-45] Notably, our case displayed a microdeletion neighboring *MYC* and loss of *CDKN2A/B* at 9p21, a known poor prognostic factor in tumor.[46] We presume that a focal del(8)(q24q24) could activate *MYC* by e.g., loss of negative regulatory elements upstream of the gene. Although clinical data of the EEF1G-ALK-positive cases reported by Palacios et al.[33], are not available, we believe that an aggressive clinical course and unfavorable prognosis of certain ALK+ ALCL is not determined by the type of ALK fusion, but rather by secondary hits affecting potent oncogenes and tumor suppressor genes (e.g. *MYC, TP53, PRDM1 and CDKNA2/B*).[32,44,45,47]

In summary, we investigated eight recently diagnosed cases of ALK+ ALCL with a cytoplasmic-only expression of ALK and identified one novel *EEF1G-ALK* rearrangement and three already known fusions, *RNF213-ALK, TPM3-ALK* and *ATIC-ALK*. Occurrence of the latter rearrangement in four out of eight (50%) studied cases confirms that *ATIC-ALK* is the most prevalent variant fusion in ALK+ ALCL. Importantly, *RNF213-ALK, TPM3-ALK* and *ATIC-ALK* fusions were recurrently present in two or more copies, contrasting with the *NPM1-ALK* chimeric gene, constantly occurring in one copy. Our functional studies show that ALK+ ALCL driven by *ATIC-ALK* compensates the weak expression and possibly weak oncogenic properties of this variant ALK fusion by an increased gene dosage. We propose a similar explanation for the copy number gain of *RNF213-ALK and TPM3-ALK*. Altogether,

our findings support the hypothesis that the transforming capacities of ALK fusions depend on the biological features of the partner genes.[48]

References

1. Swerdlow SH, Campo E, Harris NL, et al. Classification of Tumours of Haematopoietic and Lymphoid Tissues. 4th ed. Lyon, France: International Agency for Research on Cancer: 2008.
2. Morris SW, Kirstein MN, Valentine MB, et al. Fusion of a kinase gene, ALK, to a nucleolar protein gene, NPM, in non-Hodgkin's lymphoma. Science. 1994;263(5151):1281-1284.
3. Chiarle R, Gong JZ, Guasparri I, et al. NPM-ALK transgenic mice spontaneously develop T-cell lymphomas and plasma cell tumors. Blood. 2003;101(5):1919-1927.
4. Kuefer MU, Look aT, Pulford K, et al. Retrovirus-mediated gene transfer of NPM-ALK causes lymphoid malignancy in mice. Blood. 1997;90(8):2901-2910.
5. Lange K, Uckert W, Blankenstein T, et al. Overexpression of NPM-ALK induces different types of malignant lymphomas in IL-9 transgenic mice. Oncogene. 2003;22(4):517-527.
6. Lamant L, Dastugue N, Pulford K, Delsol G, Mariame B. A new fusion gene TPM3-ALK in anaplastic large cell lymphoma created by a (1;2)(q25;p23) translocation. Blood. 1999;93(9):3088-3095.
7. H Hallberg B, Palmer RH. Mechanistic insight into ALK receptor tyrosine kinase in human cancer biology. Nat Rev Cancer. 2013;13(10):685-700.
8. Falini B, Pileri S, Zinzani PL, et al. ALK+ lymphoma: clinico-pathological findings and outcome. Blood. 1999;93(8):2697-2706.
9. Boi M, Zucca E, Inghirami G, Bertoni F. Advances in understanding the pathogenesis of systemic anaplastic large cell lymphomas. Br J Haematol. 2015;168(6):771-783.
10. Drexler HG, Gignac SM, von WR, Werner M, Dirks WG. Pathobiology of NPM-ALK and variant fusion genes in anaplastic large cell lymphoma and other lymphomas. Leukemia. 2000;14(9):1533-1559.
11. Stein H, Foss Hd, Du H, et al. CD30+ anaplastic large cell lymphoma : a review of its histopathologic, genetic, and clinical features. Blood. 2000;96(12):3681-3695.

12. Sakamoto K, Nakasone H, Togashi Y, et al. ALK-positive large B-cell lymphoma: identification of EML4-ALK and a review of the literature focusing on the ALK immunohistochemical staining pattern. Int J Hematol. 2016;103(4):399-408.
13. Mologni L. Inhibitors of the anaplastic lymphoma kinase. Expert Opin Investig Drugs. 2012;21(7):985-994.
14. Pall G. The next-generation ALK inhibitors. Curr Opin Oncol. 2015;27(2):118-124.
15. Kwak EL, Bang YJ, Camidge DR, et al. Anaplastic lymphoma kinase inhibition in non-small-cell lung cancer. N Engl J Med. 2010;363(18):1693-1703.
16. Gambacorti PC, Farina F, Stasia A, et al. Crizotinib in advanced, chemoresistant anaplastic lymphoma kinase-positive lymphoma patients. J Natl Cancer Inst. 2014;106(2):djt378.
17. Cools J, Wlodarska I, Somers R, et al. Identification of novel fusion partners of ALK, the anaplastic lymphoma kinase, in anaplastic large-cell lymphoma and inflammatory myofibroblastic tumor. Genes Chromosomes Cancer. 2002;34(4):354-362.
18. Hernandez L, Bea S, Bellosillo B, et al. Diversity of genomic breakpoints in TFG-ALK translocations in anaplastic large cell lymphomas: identification of a new TFG-ALK(XL) chimeric gene with transforming activity. Am J Pathol. 2002;160(4):1487-1494.
19. Wlodarska I, De Wolf-Peeters C, Falini B, et al. The cryptic inv(2)(p23q35) defines a new molecular genetic subtype of ALK-positive anaplastic large-cell lymphoma. Blood. 1998;92(8):2688-2695.
20. Mathew P, Sanger WG, Weisenburger DD, et al. Detection of the t(2;5)(p23;q35) and NPM-ALK fusion in non-Hodgkin's lymphoma by two-color fluorescence in situ hybridization. Blood. 1997;89(5):1678-1685.
21. Perkins SL, Pickering D, Lowe EJ, et al. Childhood anaplastic large cell lymphoma has a high incidence of ALK gene rearrangement as determined by immunohistochemical staining and fluorescent in situ hybridisation: a genetic and pathological correlation. Br J Haematol. 2005;131(5):624-627.
22. Cataldo KA, Jalal SM, Law ME, et al. Detection of t(2;5) in anaplastic large cell lymphoma: comparison of immunohistochemical studies, FISH, and RT-PCR in paraffin-embedded tissue. Am J Surg Pathol. 1999;23(11):1386-1392.

23. Finalet Ferreiro J, Rouhigharabaei L, Urbankova H, et al. Integrative genomic and transcriptomic analysis identified candidate genes implicated in the pathogenesis of hepatosplenic T-cell lymphoma. PloS One. 2014;9(7):e102977.
24. Atak ZK, Gianfelici V, Hulselmans G, et al. Comprehensive analysis of transcriptome variation uncovers known and novel driver events in T-cell acute lymphoblastic leukemia. PLoS Genet. 2013;9(12):e1003997.
25. Ma Z, Cools J, Marynen P, et al. Inv(2)(p23q35) in anaplastic large-cell lymphoma induces constitutive anaplastic lymphoma kinase (ALK) tyrosine kinase activation by fusion to ATIC, an enzyme involved in purine nucleotide biosynthesis. Blood. 2000;95(6):2144-2149.
26. Colleoni GW, Bridge JA, Garicochea B, Liu J, Filippa DA, Ladanyi M. ATIC-ALK: A novel variant ALK gene fusion in anaplastic large cell lymphoma resulting from the recurrent cryptic chromosomal inversion, inv(2)(p23q35). Am J Pathol. 2000;156(3):781-789.
27. Takeoka K, Okumura A, Honjo G, Ohno H. Variant Translocation Partners of the Anaplastic Lymphoma Kinase (ALK) Gene in Two Cases of Anaplastic Large Cell Lymphoma , Identified by Inverse cDNA Polymerase Chain Reaction. J Clin Exp Hematop. 2014;54(3):225-235.
28. Siebert R, Gesk S, Harder L, et al. Complex variant translocation t(1;2) with TPM3-ALK fusion due to cryptic ALK gene rearrangement in anaplastic large-cell lymphoma. Blood. 1999;94(10):3614-3617.
29. Hoshino A, Nomura K, Hamashima T, et al. Aggressive transformation of anaplastic large cell lymphoma with increased number of ALK-translocated chromosomes. Int J Hematol. 2015;101(2):198-202.
30. Meech SJ, McGavran L, Odom LF, et al. Unusual childhood extramedullary hematologic malignancy with natural killer cell properties that contains tropomyosin 4--anaplastic lymphoma kinase gene fusion. Blood. 2001;98(4):1209-1216.
31. Liang X, Meech SJ, Odom LF, et al. Assessment of t(2;5)(p23;q35) translocation and variants in pediatric ALK+ anaplastic large cell lymphoma. Am J Clin Pathol. 2004;121(4):496-506.
32. Abate F, Todaro M, van der Krogt J, et al. A novel patient derived tumorgraft model with TRAF1-ALK anaplastic large cell lymphoma translocation. Leukemia. 2014;(6):1-32.

33. Palacios G, Shaw TI, Li Y, et al. Novel ALK fusion in anaplastic large cell lymphoma involving EEF1G, a subunit of the eukaryotic elongation factor-1 complex. Leukemia. 2017;31(3):743-747.
34. Ries S, Rnjak L, Mitrovic Z, Kuvezdic KG, Nola M, Sucic M. CD13+ anaplastic large cell lymphoma with leukemic presentation and additional chromosomal abnormality. Diagn Cytopathol. 2010;38(2):141-146.
35. Giuriato S, Foisseau M, Dejean E, et al. Conditional TPM3-ALK and NPM-ALK transgenic mice develop reversible ALK-positive early B-cell lymphoma/leukemia. Blood. 2010;115(20):4061-4070.
36. Kumabe T, Sohma Y, Yamamoto T. Human cDNAs encoding elongation factor 1 gamma and the ribosomal protein L19. Nucleic Acids Res. 1992;20(10):2598.
37. Achilonu I, Siganunu TP, Dirr HW. Purification and characterisation of recombinant human eukaryotic elongation factor 1 gamma. Protein Expr Purif. 2014;99:70-77.
38. Chi K, Jones DV, Frazier ML. Expression of an elongation factor 1 gamma-related sequence in adenocarcinomas of the colon. Gastroenterology. 1992;103(1):98-102.
39. Ender B, Lynch P, Kim YH, Inamdar NV, Cleary KR, Frazier ML. Overexpression of an elongation factor-1 gamma-hybridizing RNA in colorectal adenomas. Mol Carcinog. 1993;7:18-20.
40. Lew Y, Jones DV, Mars WM, Evans D, Byrd D, Frazier ML. Expression of elongation factor-1 gamma-related sequence in human pancreatic cancer. Pancreas. 1992;7:144-152.
41. Mimori K, Mori M, Inoue H, et al. Elongation factor 1 gamma mRNA expression in oesophageal carcinoma. Gut. 1996;38(1):66-70.
42. Van Roosbroeck K, Wlodarska I. Oncogenic Anaplastic Lymphoma Kinase Rearrangements in Lymphoma. European Haematology. 2009;3:50-56.
43. Moritake H, Shimonodan H, Marutsuka K, Kamimura S, Kojima H, Nunoi H. C-MYC rearrangement may induce an aggressive phenotype in anaplastic lymphoma kinase positive anaplastic large cell lymphoma: Identification of a novel fusion gene ALO17/C-MYC. Am J Hematol. 2011;86(1):75-78.

44. Liang X, Branchford B, Greffe B, et al. Dual ALK and MYC rearrangements leading to an aggressive variant of anaplastic large cell lymphoma. J Pediatr Hematol Oncol. 2013;35(5):e209-e213.
45. Monaco S, Tsao L, Murty VV, et al. Pediatric ALK+ anaplastic large cell lymphoma with t(3;8)(q26.2;q24) translocation and c-myc rearrangement terminating in a leukemic phase. Am J Hematol. 2007;82(1):59-64.
46. LaPak KM, Burd CE. The molecular balancing act of p16(INK4a) in cancer and aging. Mol Cancer Res. 2014;12(2):167-183.
47. Boi M, Rinaldi A, Kwee I, et al. PRDM1/BLIMP1 is commonly inactivated in anaplastic large T-cell lymphoma. Blood. 2013;122(15):2683-2693.
48. Armstrong F, Duplantier MMl, Trempat P, et al. Differential effects of X-ALK fusion proteins on proliferation, transformation, and invasion properties of NIH3T3 cells. Oncogene. 2004;23(36):6071-6082.

Table 1. Relevant clinical and pathological data.

Case	Sex/Age at diagnosis	Sites of involvement, Ann Arbor stage	Immunophenotype	Histology	Treatment	Outcome	Survival (months)	Status (A/D)
1	M/5	skin, supra and infradiaphragmatic lymph nodes. Stage IV.	CD3-, CD20-, CD30+, CD4 partial, CD8-, ALK(cyto)+ , TIA1+, perforin +, granzyme B focal +	lymphohistiocytic subtype	sequential polychemotherapy (ALCL 99 protocol, high risk);1st R: ALCL relapse protocol, BEAM + auto SCT; 2nd R: weekly vinblastine until 1,5 year; 3rd R: daily crizotinib + weekly vinblastine followed by MUD allo SCT	1st R 8 mo AD; 2nd R: 15 mo AD; 3rd R: 61 mo AD	72	D in CR (toxic death: severe GVHD, respiratory failure)
2	M/55	lymph nodes (neck). Stage III.	CD3-, CD20-, CD30+, CD5-, CD10-, prekeratin-, EMA-, CD2-, CD4+, CD7-, CD8-, TIA1-, granzymB-, perforin+, ALK(cyto)+, EBV-, bcl2 weak+, CD43-	classical morphology of ALCL	8 CHOP; 1st R: 4 DHAP; BEAM + auto SCT	CR after CHOP; R: CR after DHAP	63	A
3	F/49	lymph nodes (axillary). Stage I.	CD2-, CD3-, CD20-, PAX5-, CD15-, CD30+, CD4+, CD8-, CD5-, MUM1+, ALK(cyto)+, TIA1-, granzymeB-, perforin+, EBV-, EMA+	intrasinusoidal growth, numerous plasma cells and eosinophils in the background	N CHOP	CR	20	A
4	M/77	lymph nodes (neck). Stage I.	CD2-, CD30+, CD4-, CD8-, ALK(cyto)+,TIA1-, granzymeB-, perforin+, EMA+, weak CD138, PAX5-, IgA-, HHV8-, CD7-, CD45-, CD79a-	classical morphology of ALCL, foci of necrosis; histiocytes in background	6 CHOP	CR	24	A
5	M/52	lymph nodes (mesenteric). Stage IIA.	CD30+, CD4+, CD8-, ALK(cyto)+, TIA1+, perforin+, granzymeB+, EBV-,EMA+	large multinuclear cells with nucleoli; polymorphic stromal reactions with numerous plasma cells, neutrophils and eosinophils	8 CHOP	CR	45	A

6	F/78	Bone, supra and infra diaphragmatic lymph nodes Stage IVB	CD30+, ALK (cyto) +, CD45+, CD4+, CD20 weak+, Pax5 weak+, CD3-, CD5-, CD2-, CD8- Perforin+, granzyme+, EMA+, TIA1-	classical morphology of ALCL	8 CHOP	CR	14	A
7	M/65	lymph nodes (neck, axillary, retoroperitoneal, iliacal). Stage IIIa.	CD30+, CD15 false +, CD20-, CD3-, misdiagnosed as classical Hodgkin. Performed in 2016 after recurrence: PAX5-, CD2-, CD4-, CD8-, ALK(cyto)+, TIA1+ (partial), perforin+, granzymeB+ (partial), EBV-	Nodular sheet-like proliferation of immunoblastic to anaplastic cells; prominent intrasinusoidal localization; similar at recurrence, plus prominent histiocytic response with erythrophagocytosis and emperipolesis	2002: (initially misdiagnosed as classical Hodgkin): 6 ABVD + RT at left cervical and axillar region (30 Gy). Relapse in February 2016: stadium IVB (neck, supra- and infradiaphragmatic lymph nodes, lung (subpleural lesions)). 8 CHOP (3 received).	R: 168 mo AD	166	D
8	F/13	lymph nodes (infradiaphragmatic : retroperitoneal, iliacal) Stage IIA	CD30+, ALK (cytoplasmic, membraneous)+, EMA+, TIA1+, perforin+, GranzymeB+, CD4+ (weak), CD20-, CD3-	Diffuse parenchymal and pseudo-cohesive intrasinusoidal spread of characteristic Hallmark cells. No prominent stromal reaction.	ALCL 99 protocol: 6 courses of polychemotherapy	CR	14	A

abbreviations: M, male; F, female; R, relapse; SCT, stem cell transplantation; ABVD, doxorubicin, bleomycin, vinblastine, dacarbazine; CHOP, cyclophosphamide-adriamycin-vincristine-prednisone; DHAP, dexamethasone-cytarabine-cisplatin; BEAM, carmustine-etoposide-cytarabine- melphalan; MUD, matched unrelated; RT, radiotherapy; N, number of cycles unknown; CR, complete response; AD , after diagnosis; D, died; A, alive; GVHD, graft versus host disease

Table 2. Results of cytogenetic and molecular studies

Case	Sample/ status	Cytogenetics	aCGH profile	FISH		ALK fusion	
				LSI ALK	Other probes	partner gene (localization)	detected by
1[a]	LN/P	44-47,XY,-Y,del(2)(p23),-5[3], der(6)t(5;6)(q22;p25),add(8)(p23)[3],-9, del(10)(q25),der(11)(?::11pter->q12.3::2p23-> 2pter::2pter->p23::11q12.3->q11::q13.5-> 23.1::?),add(12)(q24)[3],+16[2],+1-4mar[4]	gains: 1q21.3q44, 2p23.2p25.3, 5q15q35.3, 6p22.2p25, 11q11q13.4, 20q13.1q13.33, 22q13.1q13.33 losses: 8q24q24,9p21.3p24.3, 10q25.3q25, 11q22.3q25	ish: 2p(F),der(2)(G), der(11)(Rx2); nuc ish:1F,1G,2R (85%)	WCP2:2+,del(2p)+,der(11)+; WCP11:11+,der11+; 5'EEF1G-SO/3'ALK-SG:2F1R1G; LSI MYC: 8F,8GRdim	*EEF1G* (11q12.3)	5'RACE PCR
2[a]	LN/D	NM	gains: 1q21.3q44, 2p23.2p25.3, 4p12p16, 5q33.3q35.3, 6, 12q15q23.2, 16p11.2p13.3, 17q23.3q25.3, 21q11.2q22.3 losses: 1p36.2p36.3, 5q15q21.2, 18q11.2q23	nuc ish:1-3F,1-3G,1-7R (19%)	RFN213 BA:3F3-7R3-7G; 5'RFN213-SO/3'ALK-SG:3-7F2-3R2-3G; RNF212 BA:5-7G ITK BA: 5-7R 5'RNF SO/3'ITK-SG: 5-7R5-7G	*RFN213* (17q25.3)	LCFGS
3[b]	LN/D	ND	ND	nuc ish:1-2F,1-2G,5-7R (16%)	ATIC BA: variable pattern with gain of red signals; 5'ATIC-SO/3'ALK- SG: 2-5F and variable R/G signals	*ATIC* (2q35)	FISH
4[b]	LN/D	ND	ND	nuc ish: 1F,1G,5R (15%)	ATIC BA: variable pattern with gain of red signals; 5'ATIC-SO/3'ALK- SG: 2-5F and variable R/G signals	*ATIC* (2q35)	FISH

5[b]	LN/D	ND	ND	nuc ish:1-3F,1-2G,3-5R (21%)	ATIC BA: variable pattern with gain of red signals; 5'ATIC-SO/3'ALK- SG: 2-5F and variable R/G signals	*ATIC* (2q35)	FISH
6[a]	LN/D	NM	ND	nuc ish:1-2F,1-3G,3-5R (9%)	ATIC BA: variable pattern with gain of red signals; 5'ATIC-SO/3'ALK- SG: 2-5F and variable R/G signals	*ATIC* (2q35)	FISH
7[a]	LN/D	88-89,XXY,-Y,i(1)(q10),+i(1)(q10),del(2)(p11),+del(2)(p11),+del(2)(p23)x2,-4,-5,-8,-8,-11,-15,-15,-18,-18,+20[2],+20[2],-21,-22[2],+2-6mar[cp3]	ND	nuc ish:2-5F,1-2G, 5-6R (15%)	TPM3 BA: 1-2F5(RsepG); 5'TPM3-S0/3'ALK-SG: 1-2R1-3G5F	*TPM3* (1q21.3)	FISH
	LN/P	47,XY,ins(1;2)(q21.3;p23p25),+ider(1)(q10)ins(1;2)(q21.3;p23p25),del(2)(p23)[2]	ND	nuc ish:1F,1G,3R (24%)	TPM3 BA: 1F3(RsepG); 5'TPM3-S0/3'ALK-SG: 1R1G3F		
8	LN/D	88,XX,-X,-X,-1,add(1)(q44),+2,-3,add(4)(p16),+5,+7,-11,+12,-13,-15,-16,+i(17)(q10),-19,-20[1]	ND	2F,4xdel(2)(p23p?)R Nuc ish:1F4R (11%)	TPM3 BA: 2F4R; 5'TPM3-S0/3'ALK-SG:2R1G4F	*TPM3* (1q21.3)	TLA

abbreviations: LN, lymph node; D, diagnosis; P, progression; NM, no mitosis, ND, not done; ish, in situ hybridization; nuc ish, interphase in situ hybridization; F, fused ; G, green, R, red; BA, break apart; RACE PCR, rapid amplification of cDNA ends; LCFGS, low coverage full genome sequencing; TLA, Targeted Locus Amplification technology (http://www.cergentis.com/tla-technology)

a, FISH performed on cytogenetic specimen; b, FISH performed on FFPE material

Legend to the figures

Figure 1. Cytogenetic and molecular analysis of case 1. (A) Examples of FISH experiments with LSI ALK and LSI MYC break apart probes. Metaphase FISH demonstrated break apart LSI ALK pattern associated with a duplication of the red/3'*ALK* signal on der(11) (left image). Paints for chromosomes 2 (red) and 11 (green) confirmed insertion of 2p23p25 at 11q12 (inset). The same aberrant LSI ALK pattern (one colocalized-one green-two red signals) was observed in interphase cells (middle image). Metaphase FISH with LSI MYC showed a diminished red signal on der(8), confirming a focal deletion at 8q24.21 (right image). (B) Schematic representation of the EEF1G, ALK and EEF1G-ALK protein structures (upper panel). Sequencing of the fragment amplified by *EEF1G-ALK* nested RT-PCR identified an in-frame fusion between exon 8 of *EEF1G* (breakpoint between exon 8 and 9) and exon 20 of *ALK* (breakpoint in the middle of exon 20) as shown in the electropherogram (lower panel). (C) Array CGH profile of case 1 showing several unbalanced regions, including gain of 2p23pter and 11q11q13.4 (marked). (D) The selected 2pter (upper panel) and 11q (lower panel) regions. Note the 2p23pter gain-associated break within the ALK gene (gain of 3'ALK) and localization of *EEF1G* in the middle of gained 11q11q13.4 region.

Figure 2. Cytogenetic and molecular analysis of case 2. (A) Examples of interphase FISH experiments. Note a break apart pattern of LSI ALK and RNF213 BA probes associated with gain of six 3'*ALK* (red) signals (left image) and six 5'*RNF213* (red) signals (middle image). Several colocalized 5'*RNF213* (red) and the 3'*ALK* (green) signals in interphase cells confirm presence and gain of the *RNF213-ALK* hybrid gene in this case (left image). (B) Schematic representation of the RNF213, ALK and RNF213-ALK protein structures (upper panel). Low coverage full genome sequencing resulted in at least eight single read pairs covering the in-frame fusion between exon 8 of *RNF213* and exon 20 of *ALK* (lower panel). (C) Array CGH profile of case 2 showing several unbalanced regions, including gains of 2p23pter and 17q23qter (marked). (D) The selected 2p23pter (upper panel) and 17q23qter (lower panel) regions evidencing the gain-associated breaks within the *ALK* and *RNF213* genes, respectively.

Figure 3. Cytogenetic and FISH analysis of cases 3, 7 and 8. (A-C) Note a break apart pattern of LSI ALK and ATIC BA probes associated with a gain of four 3'*ALK* (red) and four 5'*ATIC* (red) signals, respectively, in case 3. Several colocalized 5'*ATIC*/3'*ALK* signals in interphase cells demonstrate gain of the *ATIC-ALK* hybrid gene in this sample. Similar FISH results were obtained in cases 4 and 5. Case 7: (D) Partial karyotype (at time of relapse) illustrating insertion of 2p23p25 at 1q21.3 (arrowhead), isochomosome 1q containing duplicated long arm of ins(1;2)(q21.3;p23q25) (two arrowheads) and del(2)(p23) (arrow). (E) Note rearrangement of *ALK* and gain of two extra 3'*ALK* (red) signals, and (F) three separated red and green TPM3 BA probes, likely marking ins(1) and ider(1). (G-I) Similar FISH patterns were observed in the diagnostic sample. Case 8: (J) Note four copies of der(2) marked by red signals of LSI ALK, (K) unbalanced rearrangement of *TPM3* and (L) loss of *TPM3* from one chromosome 1 and four copies of der(2)/*TPM3-ALK*.

Figure 4. Functional analysis of the NPM1-, EEF1G-, RNF213-, TPM3- and ATIC-ALK fusions. (A) Expression analysis of the five ALK partner genes using previously generated RNA-sequencing data[23,24] In contrast to *EEF1G*, expression of *TPM3*, *RNF213,* and *ATIC* is significantly lower (p-value <0,001) when compared to *NPM1* in different malignant and non-malignant cell types (HSTL = hepatosplenic T-cell lymphoma (n=4), T-ALL = T-cell acute lymphoblastic leukemia (n=5), PTCL = peripheral T-cell lymphoma (n=2), Spleen (n=1), Thymus (n=1), LN = lymph nodes (n=3), Th1 (n=5), Th2 (n=5), Treg (n=5), and CD4 naïve T-cells (n=4)). Error bars represent the standard deviation (SD). (B) QRT-PCR on Ba/F3 Cas9 cells showing the expression levels of *Npm1* and *Atic*. The expression of *Atic* is significantly lower than *Npm1* (p<0,001). Error bars represent the SD. (C) Representation of the *Alk, Npm1,* and *Atic* mouse genes. Exons are indicated by vertical bars. Red arrows indicate the location of the gRNA target sites. (D) Growth curve showing the transforming capacities of Ba/F3 Cas9 cells harboring an endogenous Npm1-Alk or Atic-Alk fusion. Error bars represent the SD. (E) Growth curve showing the growth rate of Ba/F3 Cas9 cells after transformation by the endogenous Alk fusion. Error bars represent the SD. (F-H) Examples of metaphase and interphase FISH results showing the endogenous Alk fusions in Ba/F3 Cas9 cells. Arrows point colocalized signals/chimeric genes. Note a constant presence of a single copy of *Npm1-Alk* and gain of *Atic-Alk* in late cultures.

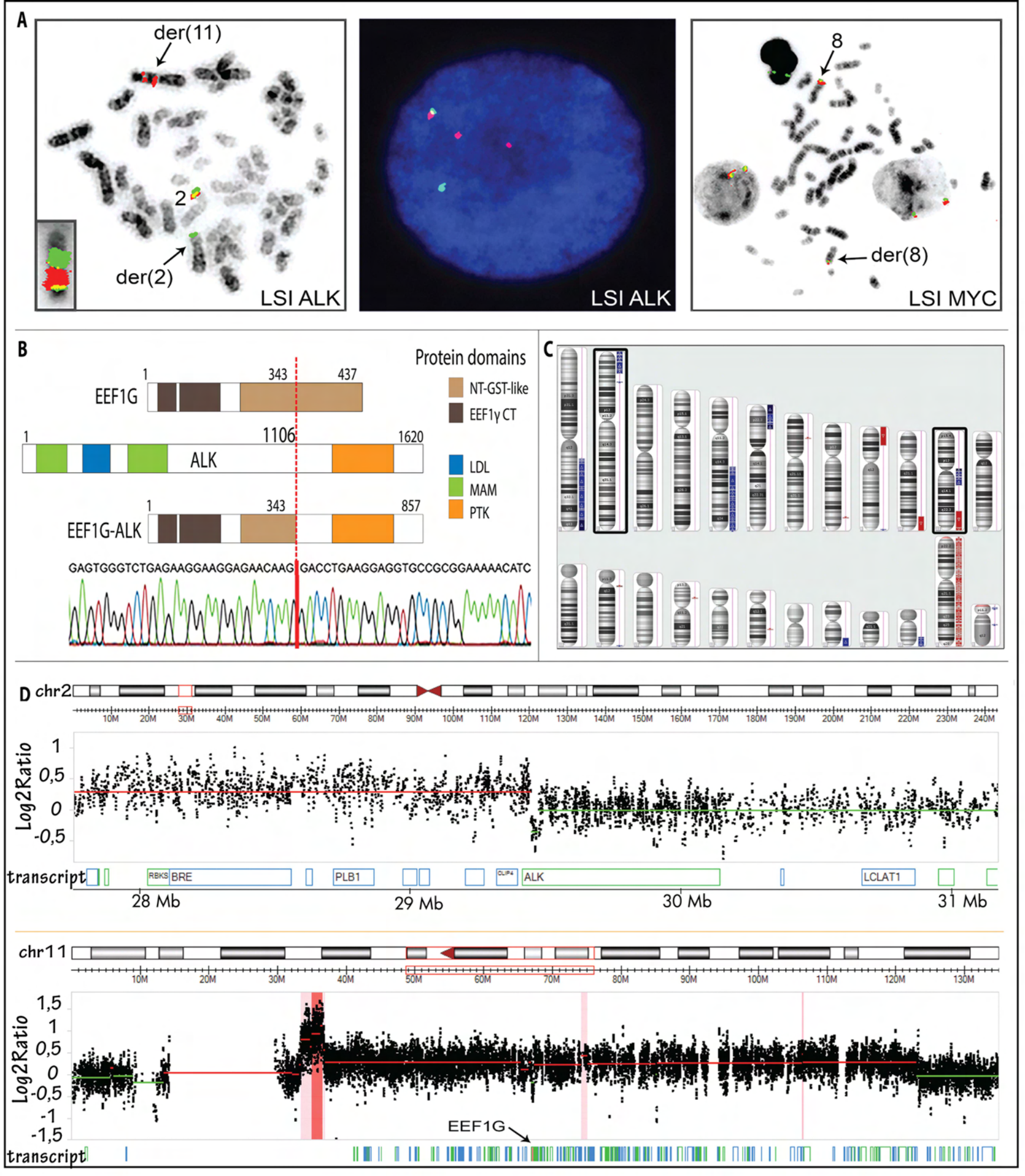
A
der(11)
2
der(2)
LSI ALK
LSI ALK
8
der(8)
LSI MYC
B
Protein domains
NT-GST-like
EEF1γ CT
LDL
MAM
PTK
EEF1G
ALK
EEF1G-ALK
GAGTGGGTCTGAGAAGGAAGGAGAACAAG GACCTGAAGGAGGTGCCGCGGAAAAACATC
C
D
chr2
Log2Ratio
transcript
RBKS
BRE
PLB1
DUP4
ALK
LCLAT1
28 Mb
29 Mb
30 Mb
31 Mb
chr11
EEF1G

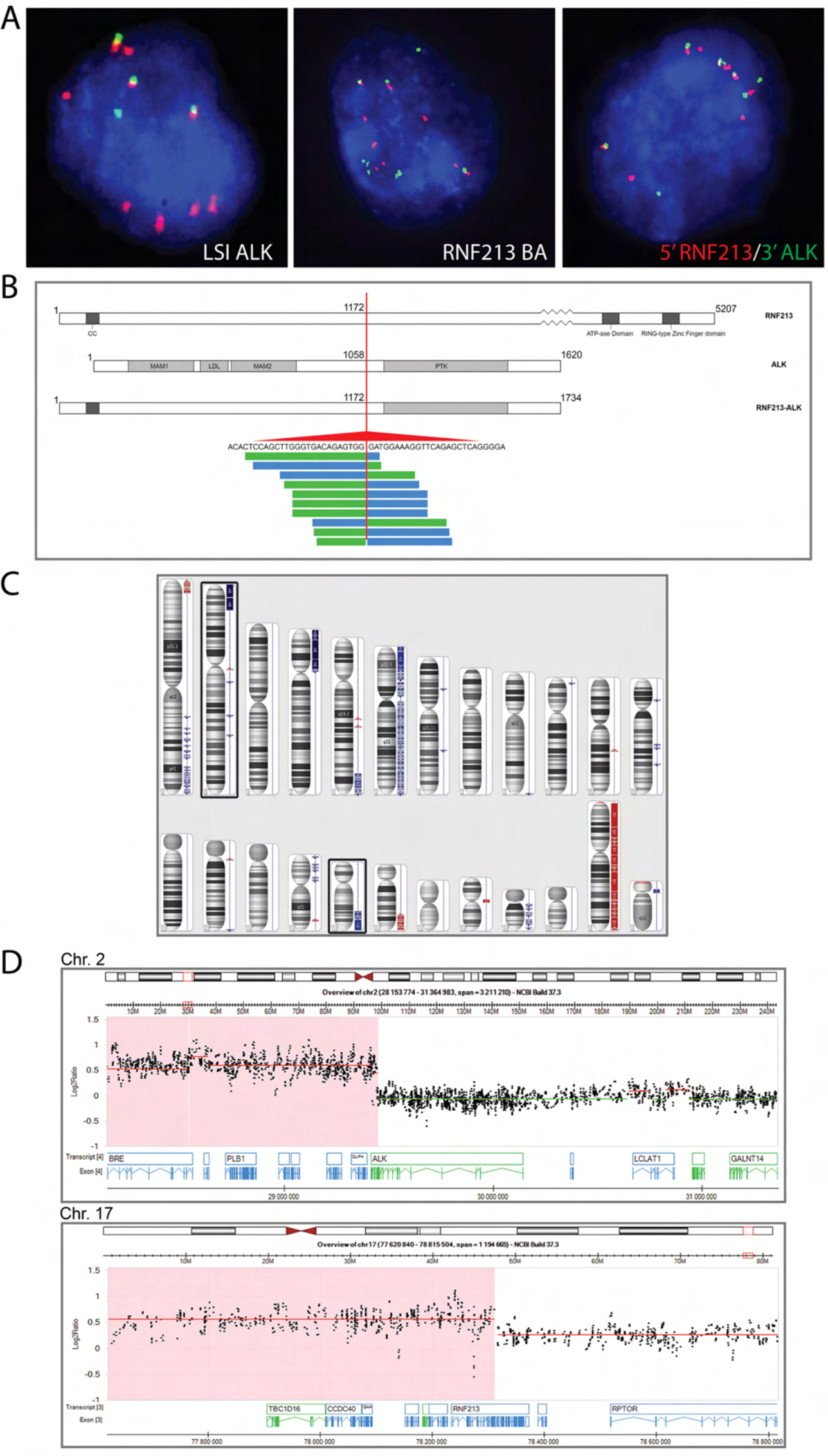
A
LSI ALK
RNF213 BA
5′ RNF213/3′ ALK
B
1
1172
5207
RNF213
CC
ATP-ase Domain
RING-type Zinc Finger domain
1
1058
1620
ALK
MAM1
LDL
MAM2
PTK
1
1172
1734
RNF213-ALK
ACACTCCAGCTTGGGTGACAGAGTGG
GATGGAAAGGTTCAGAGCTCAGGGGA
C
D
Chr. 2
Overview of chr2 (28 153 774 - 31 364 983, span = 3 211 210) - NCBI Build 37.3
Log2Ratio
Transcript [4]
Exon [4]
BRE
PLB1
ALK
LCLAT1
GALNT14
29 000 000
30 000 000
31 000 000
Chr. 17
Overview of chr17 (77 620 840 - 78 815 504, span = 1 194 665) - NCBI Build 37.3
Log2Ratio
Transcript [3]
Exon [3]
TBC1D16
CCDC40
RNF213
RPTOR
77 800 000
78 000 000
78 200 000
78 400 000
78 600 000
78 800 000

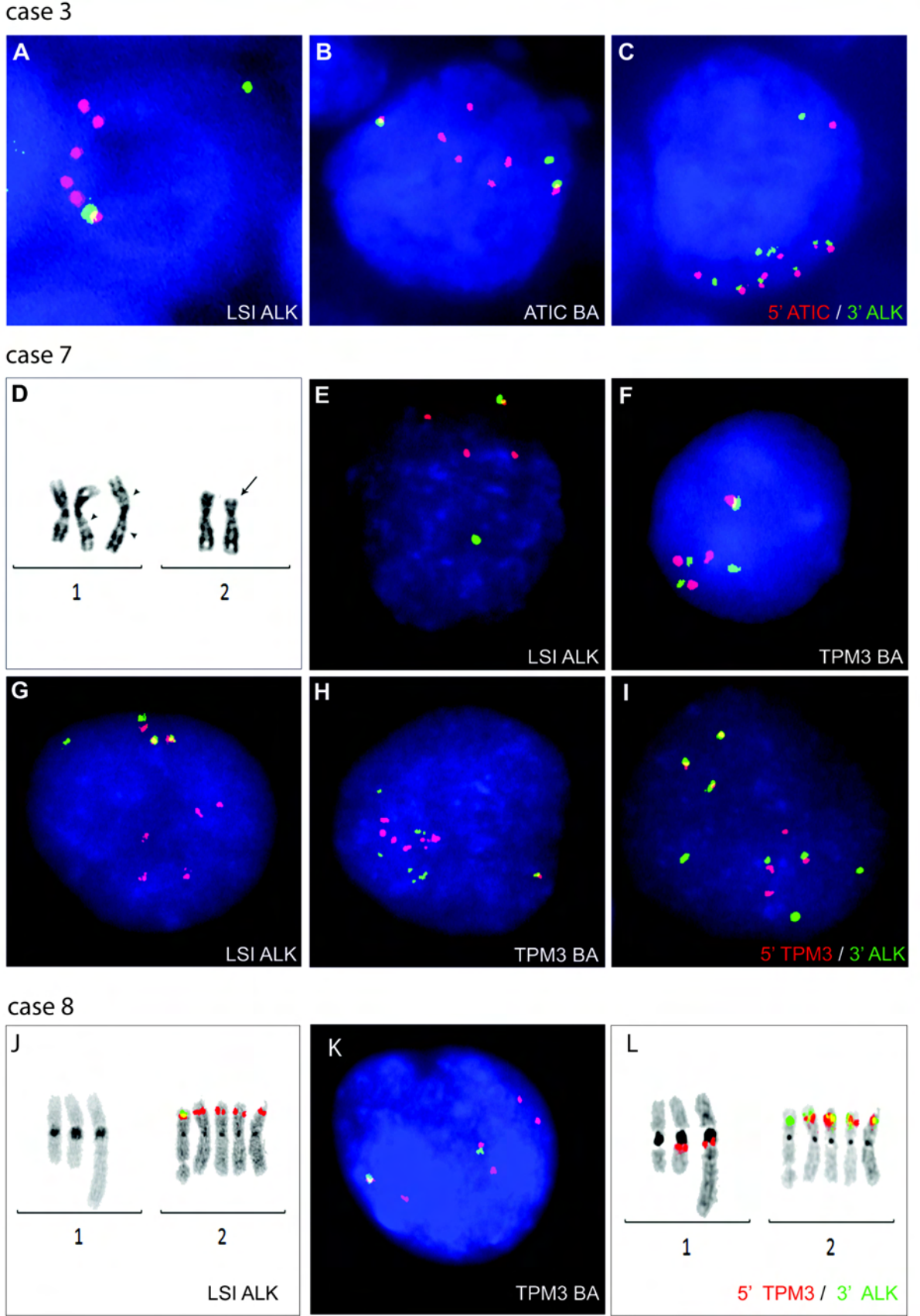
case 3
A
LSI ALK
B
ATIC BA
C
5' ATIC / 3' ALK
case 7
D
1
2
E
LSI ALK
F
TPM3 BA
G
LSI ALK
H
TPM3 BA
I
5' TPM3 / 3' ALK
case 8
J
1
2
LSI ALK
K
TPM3 BA
L
1
2
5' TPM3 / 3' ALK

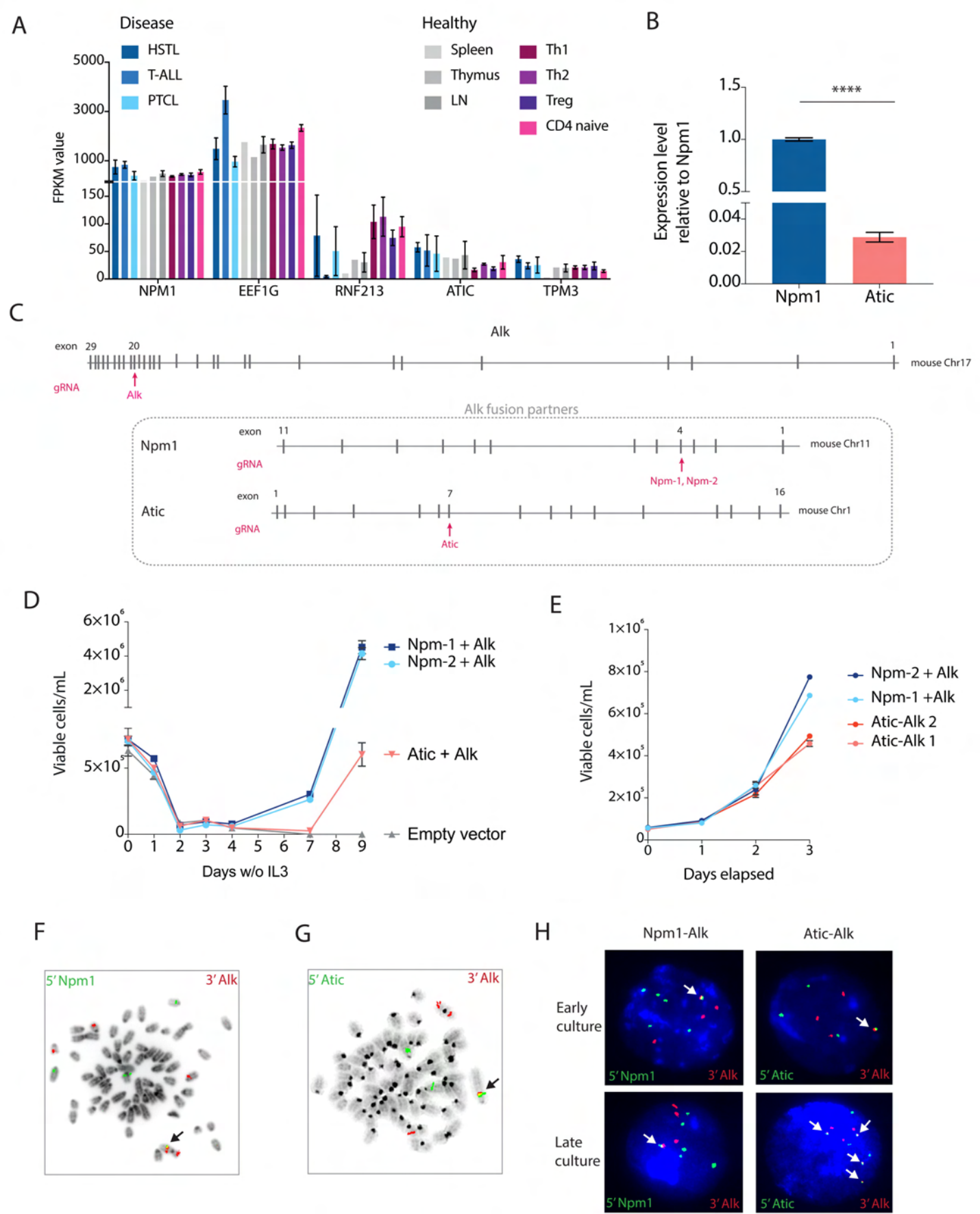
A
Disease
HSTL
T-ALL
PTCL
Healthy
Spleen
Thymus
LN
Th1
Th2
Treg
CD4 naive
FPKM value
5000
3000
1000
150
100
50
0
NPM1
EEF1G
RNF213
ATIC
TPM3
B
Expression level relative to Npm1
1.5
1.0
0.5
0.04
0.02
0.00
****
Npm1
Atic
C
Alk
exon 29
20
1
mouse Chr17
gRNA
Alk
Alk fusion partners
Npm1
exon 11
4
1
mouse Chr11
gRNA
Npm-1, Npm-2
Atic
exon 1
7
16
mouse Chr1
gRNA
Atic
D
Viable cells/mL
6x10^6
4x10^6
2x10^6
5x10^5
0
0 1 2 3 4 5 6 7 8 9
Days w/o IL3
Npm-1 + Alk
Npm-2 + Alk
Atic + Alk
Empty vector
E
Viable cells/mL
1x10^6
8x10^5
6x10^5
4x10^5
2x10^5
0
0 1 2 3
Days elapsed
Npm-2 + Alk
Npm-1 +Alk
Atic-Alk 2
Atic-Alk 1
F
5′ Npm1
3′ Alk
G
5′ Atic
3′ Alk
H
Npm1-Alk
Atic-Alk
Early culture
Late culture
5′ Npm1
3′ Alk
5′ Atic
3′ Alk

Supplemental information

Supplemental Methods

5' Rapid Amplification of cDNA Ends Polymerase-Chain-Reaction (RACE-PCR)

Total RNA was extracted from 20µm sections of frozen tissue samples using TRIzol Reagent (Life Technologies, Merelbeke, Belgium). With random primers and Superscript III reverse transcriptase (Invitrogen, Carlsbad, CA), one microgram of total RNA was reverse transcribed into cDNA using random hexamers and SuperScript III (Life Technologies, Merelbeke, Belgium).

5'RACE-PCR experiments were performed following a previously described protocol.[1] The used 5' RACE PCR primers are listed in the Supplemental Table 2. The final PCR products were cloned in into the pJET1.2 CloneJET vector (Thermo Fisher Scientific (Fermentas), Waltham, MA). Subsequently, Sanger sequencing of the PCR products was performed and Sanger chromatograms were analyzed using CLC Main Workbench 6 (CLC Bio Inc., Cambridge, MA).

Low coverage full genome sequencing (LCFGS)

The Illumina standard kit (Illumina® TruSeq™ DNA Sample Preparation Kit) was used for the DNA-sequencing sample preparation according to the manufacturer's protocol (Illumina, San Diego, CA). The quality of the libraries was checked by Agilent Technologies 2100 Bioanalyzer with the Agilent DNA 1000 Kit (Agilent, Santa Clara, CA). Prepared libraries were sequenced using HiSeq 2000 (Illumina) operated in paired-end 2×100 bp mode. Reads were quality-filtered using standard Illumina process. To analyze the data, the fastq files were mapped to the reference human genome (Human.B37.3) using the Ensembl gene model (Homo_sapiens.GRCh37.67). The mapping and downstream analysis were performed with the software ArrayStudio, version 6.2 (www.omicsoft.com).

Targeted Locus Amplification

Viably frozen lymphoma cells were sent to Cergentis B.V. (Utrecht, the Netherlands) for Targeted Locus Amplification (TLA) and sequencing. Sample preparation, sequencing and data analysis were performed as previously described.[2]

Nested Reverse-Transcription Polymerase-Chain-Reaction (RT-PCR)

Fusion *ALK* transcripts were validated by nested RT-PCR. First strand cDNA was prepared as described above and RT-PCR was done on a cDNA template using two rounds of conventional PCR following standard protocols that come with *Taq* DNA polymerase (Roche Diagnostics GmbH, Mannheim, Germany). The primers were designed to amplify 400-600 bp fragments containing the identified fusion boundary. Subsequently, Sanger sequencing of the PCR products was performed and Sanger chromatograms were analyzed using CLC Main Workbench 6 (CLC Bio Inc.). The primers used can be found in the Supplemental Table 2.

Supplemental Tables

Supplemental Table 1. List of FISH probes.

Supplemental Table 2. List of primers.

Supplemental Table 3. The guide RNA sequences.

Supplemental Figures

Supplemental Figure 1. Generation of Ba/F3 Cas9 expressing cells.

Supplemental Figure 2. Map of the plasmid pX321.

Supplemental Figure 3. Morphology and immunophenotype. Representative histopathology of case 1 with the novel EEF1G-ALK fusion and case 4 with the ATIC-ALK fusion. Hematoxylin and eosin staining shows an anaplastic lymphoid cell proliferation with characteristic hallmark and doughnut cells (top insets). The neoplastic cells overexpress CD30 and cytoplasmic ALK1.

Supplemental Figure 4. Results of the TLA/sequencing performed in case 8. (A) The primer sets were used in individual TLA amplifications. PCR products were purified and library prepped using the Illumina NexteraXT protocol and sequenced on an Illumina Miniseq sequencer. Reads were mapped using BWA-SW, which is a Smith-Waterman alignment tool. This allows partial mapping which is optimally suited for identifying break spanning reads. The human genome version hg19 was used for mapping. (B) TLA sequence coverage across the human genome. Data shown was generated using primer set 1 (upper panel) and set 2 (lower panel). The different chromosomes are indicated on the y-axis, the

chromosomal position on the x-axis. Encircled in blue is the position of the primer-set at ALK gene locus, in red is the fusion partner. A high coverage peak in chromosome 2 was identified at the ALK locus. An additional peak at chromosome 1 at the TPM3 gene was identified. (C) IGV screenshot showing the sequence coverage across the ALK gene human locus. Coverage generated across chr2:29,446,372-29,447,630 using primer set 1 (top panel) and set 2 (bottom panel) are depicted. Blue arrow indicates the breakpoint position. Green arrows indicate primer position. Y-axis is limited to 100x. (D) IGV screenshot showing the sequence coverage across the breakpoint at the TPM3 gene human locus. Coverage generated across chr1:154,121,228-154,168,475 using primer set 1 (top panel) and primer set 2 (bottom panel) are depicted. Blue arrow indicates the breakpoint. Y-axis is limited to 100x. (E) Results of sequencing.

References

1. Cools J, Wlodarska I, Somers R, et al. Identification of novel fusion partners of ALK, the anaplastic lymphoma kinase, in anaplastic large-cell lymphoma and inflammatory myofibroblastic tumor. Genes Chromosomes Cancer. 2002;34(4):354-362.
2. de Vree PJ, de Wit E, Yilmaz M, et al. Targeted sequencing by proximity ligation for comprehensive variant detection and local haplotyping. Nat Biotechnol. 2014;32(10):1019-1025.